XIV International Conference on Topics in Astroparticle and Underground Physics (TAUP 2015) IOP Publishing
Journal of Physics: Conference Series **718** (2016) 062045 doi:10.1088/1742-6596/718/6/062045

Characterization of the Astrophysical Neutrino Flux at the IceCube Neutrino Observatory

Lars Mohrmann for the IceCube Collaboration
DESY, Platanenallee 6, D-15738 Zeuthen, Germany
E-mail: lars.mohrmann@desy.de

Abstract. With the discovery of a high-energy astrophysical neutrino flux, the IceCube Neutrino Observatory, located at the geographical South Pole, has opened the field of high-energy neutrino astronomy. While evidence for extraterrestrial neutrinos has been found in multiple searches, it was not yet possible to identify their sources; they appear as an isotropic excess. Nevertheless, it is possible to constrain the properties of the sources by measuring the energy spectrum and the flavor composition of the flux. Here, we present the latest results from a global analysis, combining all available detection channels and energy ranges. We derive the currently most precise constraints on the energy spectrum and flavor composition of the astrophysical neutrino flux. In addition, we show projected constraints on these properties that can be obtained with additional data in the future.

1. Introduction

The discovery of a cosmic neutrino flux in the TeV–PeV energy range at the IceCube Neutrino Observatory [1] has been confirmed in a number of subsequent searches [2, 3, 4, 5]. Each of these studies was focused on a particular aspect of the flux. Recently, a combined analysis has obtained the most accurate general characterization of the flux so far [6], based on three of the mentioned studies [2, 3, 4] and on previous searches performed with data taken during the construction phase of the IceCube detector [7, 8, 9]. Here, we present the latest results from this analysis, taking into account new data [10, 11, 12]. In addition, we show projected constraints on the properties of the cosmic neutrino flux that can be obtained with more data in the future.

2. Motivation & Expectations

Cosmic neutrinos are produced in interactions of high-energy cosmic rays with matter or radiation [13]. It is expected that such interactions frequently occur within, or close to, the as yet unknown acceleration sites of the cosmic rays [14]. Candidate sites for high-energy neutrino emission include active galactic nuclei, gamma-ray bursts, and starburst galaxies, but also objects within our Galaxy, such as supernova remnants or pulsar wind nebulae [15].

Ultimately, the aim of neutrino astronomy is to resolve, and thus identify, individual sources of high-energy neutrinos. However, this is not yet possible for the observed cosmic neutrino flux; the arrival directions of the neutrinos are consistent with an isotropic flux [2, 10]. Nevertheless, it is possible to constrain the properties of the sources by measuring general characteristics of the flux, such as its energy spectrum and its composition of neutrino flavors [16, 17].

The expected energy spectrum of the cosmic neutrino flux depends on the energy spectrum of the primary cosmic rays as well as on the type of interactions and the environments of the source. If the Fermi shock acceleration mechanism is responsible for the acceleration of the cosmic rays, a power law energy spectrum with spectral index close to -2 is expected [18]. This scenario has served as a popular benchmark in the past.

The majority of cosmic neutrinos are expected to be created in the decay of charged pions and the subsequent decay of muons. In this scenario, the initial composition of neutrino flavors is $\nu_e : \nu_\mu : \nu_\tau = 1 : 2 : 0$. During propagation, the composition is transformed due to neutrino oscillations, leading to an expected composition of approximately $1 : 1 : 1$ at the Earth [17]. Other (idealized) scenarios include the sole production of muon neutrinos ($0 : 1 : 0$, $\approx 1 : 1.8 : 1.8$ at Earth) or electron neutrinos ($1 : 0 : 0$, $\approx 2.5 : 1 : 1$ at Earth) [17].

3. Detecting Neutrinos with IceCube

The IceCube Neutrino Observatory [19] is a neutrino telescope located at the geographical South Pole in Antarctica. It consists of more than 5,000 optical sensors, installed on 86 vertical strings, buried in a cubic-kilometer of glacial ice between depths of 1,450 m and 2,450 m. Neutrino interactions are recorded by detecting the Cherenkov emission of secondary particles created in the interactions. Based on the arrival time and the amount of light registered in the sensors, the energy and incoming direction of the neutrino can be inferred.

The signatures that neutrinos leave in the IceCube detector can be classified into two main categories. On the one hand, *tracks* arise from charged-current ν_μ interactions. The muons created in such interactions can travel for several kilometers, thus leaving an elongated, track-like signature. Depending on whether the interaction occurs inside or outside the instrumented volume of the detector, we distinguish *starting tracks* and *throughgoing tracks*.

On the other hand, charged-current interactions of ν_e and ν_τ and neutral-current interactions of all neutrinos lead to *showers*, which, due to their small extent with respect to the sensor spacing, exhibit a spherical hit pattern. In the past, only *contained showers* were studied, i.e. those that start well inside the detection volume. Recently, also *uncontained showers* that start near the edge of the detection volume were analyzed for the first time [12].

Charged-current interactions of ν_τ can be identified at very high energies, $\gtrsim 1$ PeV. While no ν_τ were identified yet, a new upper limit on the cosmic ν_τ flux was recently presented in [11]. The limit is derived from a search for events that exhibit *double pulse waveforms*, i.e. a double-peak structure in the time-resolved signal recorded by the sensors.

4. Analysis

The analysis presented here is a continuation of the analysis presented in [6]. The method is summarized in the following; the reader is referred to the reference for more details.

The event samples analyzed here are listed in Table 1. Where data taking periods overlap, the event samples were separated with additional criteria, thus ensuring statistical independence of all samples. Each sample provides simulated probability density functions (PDFs) as well as experimental distributions for the observables listed in the third column of the table.

Background contributions to the event samples are entirely of atmospheric origin. The contribution of atmospheric muons is estimated by simulating air showers with the CORSIKA code [20]. The background of conventional and prompt atmospheric neutrinos is taken from model calculations by Honda et al. [21] and Enberg et al. [22], respectively. The normalizations of both components are free parameters in the analysis (denoted by ϕ_{conv} and ϕ_{prompt}).

Table 1. Event selections used in this analysis. Event selections marked with an asterisk were newly added or extended with respect to the analysis presented in [6]. Note that only the sample of uncontained showers from reference [12] is used here.

ID	Signatures	Observables	Period	References
T1	throughgoing tracks	energy, zenith	2009–2010	[7]
T2	throughgoing tracks	energy, zenith	2010–2012	[4]
S1	cont. showers	energy	2008–2009	[8]
S2	cont. showers	energy	2009–2010	[9]
H1*	cont. showers, starting tracks	energy, zenith	2010–2014	[1, 2, 10]
H2	cont. showers, starting tracks	energy, zenith, signature	2010–2012	[3]
DP*	double pulse waveform	signature	2011–2014	[11]
US*	uncont. showers	energy	2010–2012	[12]

We use two different spectral hypotheses to describe the cosmic neutrino flux:

$$\begin{aligned} &\text{Hypothesis A:} \quad \Phi_\nu = \phi \times (E\,/\,100\,\text{TeV})^{-\gamma} \\ &\text{Hypothesis B:} \quad \Phi_\nu = \phi \times (E\,/\,100\,\text{TeV})^{-\gamma} \times \exp(-E/E_{\text{cut}}) \end{aligned} \tag{1}$$

where $\phi, \gamma, E_{\text{cut}}$ are free parameters, respectively. To determine the energy spectrum, we assume that the flux is composed of equal flavors at Earth. The flavor composition is then derived by varying the normalizations of all three flavors independently, assuming that their energy spectrum is identical.

Systematic uncertainties are incorporated in the analysis procedure via several nuisance parameters. The experimental data are compared to the simulated PDFs by means of a binned Poisson-likelihood analysis. The best-fit model parameter values are determined by maximizing the likelihood to obtain the observed distributions of observables in all samples simultaneously.

5. Results

The results of the analysis are summarized in Table 2. When no cut-off is present, the best-fit spectral index is 2.49 ± 0.08. If an exponential cut-off is allowed, the best-fit spectral index is $2.31^{+0.14}_{-0.15}$, and the best-fit cut-off energy is $\left(2.7^{+7.7}_{-1.4}\right)$ PeV. The hypothesis with a cut-off is slightly preferred, although with a significance of only $1.2\,\sigma$ ($p = 12\%$). Both models describe the data reasonably well. On the other hand, an unbroken power law spectrum with $\gamma = 2$ can be excluded with a significance of $4.6\,\sigma$ ($p = 0.00018\%$).

Table 2. Results for the energy spectrum. Quoted uncertainties are at $1\,\sigma$ confidence level.

Param.	Unit	Hyp. A	Hyp. B
ϕ_{conv}	HKKMS model	$1.10^{+0.20}_{-0.15}$	$1.11^{+0.20}_{-0.15}$
ϕ_{prompt}	ERS model	$0.0^{+0.7}_{-0.0}$	$0.0^{+0.8}_{-0.0}$
ϕ	$10^{-18}\,\text{GeV}^{-1}\text{s}^{-1}\text{sr}^{-1}\text{cm}^{-2}$	$7.0^{+1.0}_{-1.0}$	$8.0^{+1.3}_{-1.2}$
γ	—	$2.49^{+0.08}_{-0.08}$	$2.31^{+0.14}_{-0.15}$
E_{cut}	PeV	—	$2.7^{+7.7}_{-1.4}$
$-2\Delta \ln L$		+1.94	0

The correlation between the spectral index γ and the cut-off energy E_{cut} is visualized in fig. 1(a). Figure 1(b) shows the best-fit spectrum for both hypotheses together with a differential model that extracts the cosmic neutrino flux in separate energy intervals.

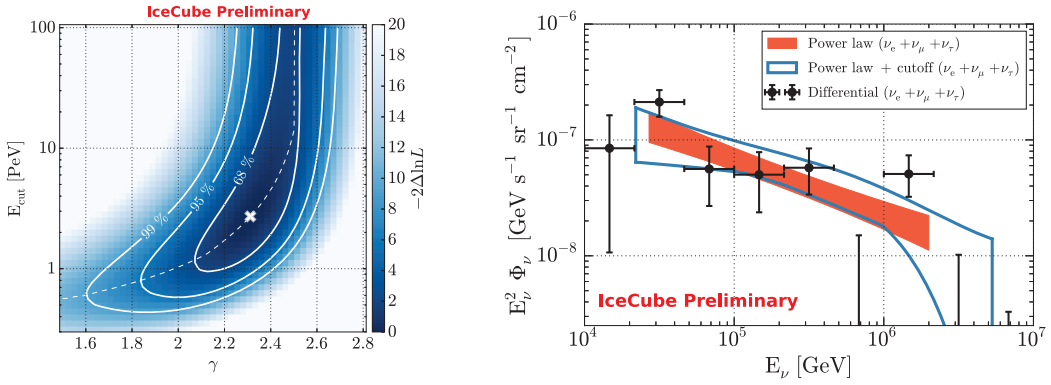

(a) (b)

Figure 1. Results on the energy spectrum. (a) Profile likelihood scan of parameters γ and E_{cut}. The best fit is marked with '×'. The dashed line shows the conditional best-fit value of E_{cut} for each value of γ. (b) Energy spectrum of the cosmic neutrino flux. Shown are the spectra allowed at 68% C.L. for hypothesis A (power law) and hypothesis B (power law + cutoff). In addition, the strength of the cosmic neutrino flux in separate energy intervals is shown (differential).

Results on the flavor composition are presented in fig. 2. For both spectral hypotheses, the flux consists of ν_e and ν_μ in approximately equal parts at the best fit. However, compositions expected for pion-decay sources ($1:2:0$ at source) and muon-damped sources ($0:1:0$ at source) are still compatible with our data. On the other hand, a flux composed purely of electron neutrinos at the source is excluded with a significance of $3.7\,\sigma$ ($p = 0.012\%$).

Almost all of the event selections can be applied to new data that are already recorded. The resulting expected sensitivity to the energy spectrum and flavor composition is investigated in the following section.

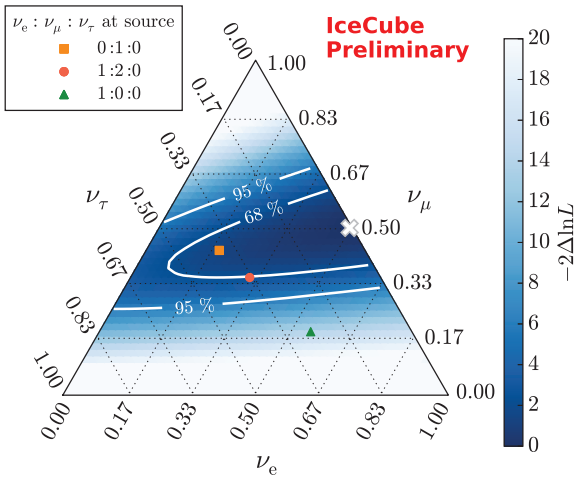

Figure 2. Results on the flavor composition. The best fit is marked with '×'. Compositions for different source scenarios are also shown.

6. Projected Sensitivities

In order to derive the future sensitivity of the IceCube detector, we use a prototype analysis that is based on the event selections of samples T2, H2, DP, and US (cf. Table 1). We weight the simulated cosmic neutrino flux to the current best-fit energy spectrum of hypothesis A or B (cf. previous section) and scale the expected signal up to mimic the collection of additional data. For the conventional and prompt atmospheric neutrino flux, we assume a flux at the level of the predictions by Honda et al. [21] and Enberg et al. [22], respectively. The sensitivity is derived using the approach described in [23].

The projected sensitivity to the energy spectrum is illustrated in fig. 3(a), where we focus on the sensitivity to the presence of an exponential high-energy cut-off to the spectrum. If no cut-off is present, the expected lower limit with 10 years of full detector data is 6.7 PeV at $2\,\sigma$ confidence. On the other hand, for a true cut-off energy at the current best fit, the non-existence of an exponential cut-off can be rejected with a significance of $\sim 3\,\sigma$ with 10 years of data.

Finally, to illustrate our future sensitivity to the flavor composition of the cosmic neutrino flux, we show the median expected constraints for 10 years of full detector data in fig. 3(b). Here, we assume an energy spectrum matching the current best fit of hypothesis B and that the cosmic neutrino flux consists of equal flavors. Although we included a search for ν_τ signatures in this analysis for the first time, a degeneracy with respect to the ν_e/ν_τ fraction remains, resulting in the elongated shape of the contours. However, the ability to distinguish between different source scenarios is largely orthogonal to this degeneracy, and thus not affected.

7. Summary

We have presented a continuation of the combined likelihood analysis of the diffuse cosmic neutrino flux presented in [6]. We find that the energy spectrum of the cosmic neutrino flux is well described by an unbroken power law, with a best-fit spectral index of -2.49 ± 0.08. This corresponds to a rejection of an unbroken power law with index -2 with $4.6\,\sigma$ significance ($p = 0.00018\%$). While the analysis slightly favors a harder power law ($E^{-2.31\pm0.15}$) with an exponential cut-off at $\left(2.7^{+7.7}_{-1.4}\right)$ PeV over an unbroken power law, the statistical significance of $1.2\,\sigma$ ($p = 12\%$) is too low to draw any conclusion. However, we have shown that the presence of a cut-off can likely be determined with additional data in the foreseeable future. Other, more complex spectral shapes are also possible, although currently not required to describe the data.

The flavor composition of the cosmic neutrino flux is compatible with standard scenarios for the neutrino production at the sources. However, a neutron-decay dominated scenario, in which

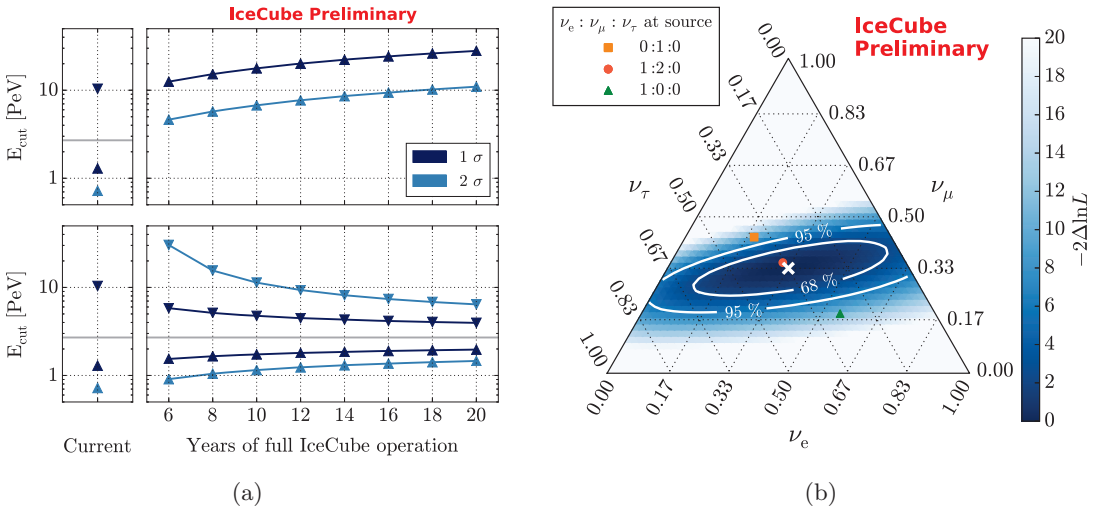

(a) (b)

Figure 3. (a) Current (small panels) and projected (large panels) constraints on the energy of an exponential cut-off to the spectrum. The two small panels show the best-fit result of hypothesis B. In the top (bottom) right panel, the best-fit spectrum of hypothesis A (B) is assumed to be true. Dark and light blue points indicate median $1\,\sigma$ and $2\,\sigma$ limits, respectively. (b) Projected sensitivity to the flavor composition, for 10 years of full detector data. The white '×' marks the assumed true flavor composition of $\nu_e : \nu_\mu : \nu_\tau = 1 : 1 : 1$.

only electron neutrinos are produced at the sources, can be ruled out with $3.7\,\sigma$ significance ($p = 0.012\%$). A projection of our sensitivity to the flavor composition has shown that while a degeneracy with respect to the ν_e/ν_τ fraction remains, a distinction between more source scenarios might be possible.

References

[1] Aartsen M G *et al* (IceCube Collaboration) 2013 *Science* **342** 1242856
[2] Aartsen M G *et al* (IceCube Collaboration) 2014 *Phys. Rev. Lett.* **113** 101101
[3] Aartsen M G *et al* (IceCube Collaboration) 2015 *Phys. Rev. D* **91** 022001
[4] Aartsen M G *et al* (IceCube Collaboration) 2015 *Phys. Rev. Lett.* **115** 081102
[5] Aartsen M G *et al* (IceCube Collaboration) 2015 *Phys. Rev. Lett.* **114** 171102
[6] Aartsen M G *et al* (IceCube Collaboration) 2015 *Astrophys. J.* **809** 98
[7] Aartsen M G *et al* (IceCube Collaboration) 2014 *Phys. Rev. D* **89** 062007
[8] Aartsen M G *et al* (IceCube Collaboration) 2014 *Phys. Rev. D* **89** 102001
[9] Schönwald A *et al* for the IceCube Collaboration 2013 *Proc. 33rd ICRC* ArXiv:1309.7003
[10] Kopper C *et al* for the IceCube Collaboration 2015 *Proc. 34th ICRC* PoS(ICRC2015)1081
[11] Williams D R *et al* for the IceCube Collaboration 2015 *Proc. 34th ICRC* PoS(ICRC2015)1071
[12] Niederhausen H M *et al* for the IceCube Collaboration 2015 *Proc. 34th ICRC* PoS(ICRC2015)1109
[13] Gaisser T K, Halzen F and Stanev T 1995 *Phys. Rep.* **258** 173–236
[14] Learned J G and Mannheim K 2000 *Annu. Rev. Nucl. Part. S.* **50** 679–749
[15] Becker J K 2008 *Phys. Rep.* **458** 173–246
[16] Lipari P, Lusignoli M and Meloni D 2007 *Phys. Rev. D* **75** 123005
[17] Choubey S and Rodejohann W 2009 *Phys. Rev. D* **80** 113006
[18] Gaisser T K 1990 *Cosmic Rays and Particle Physics* (Cambridge: Cambridge University Press)
[19] Gaisser T K and Halzen F 2014 *Annu. Rev. Nucl. Part. S.* **64** 101–123
[20] Heck D, Knapp J, Capdevielle J N, Schatz G and Thouw T 1998 *CORSIKA: a Monte Carlo code to simulate extensive air showers* Tech. Rep. FZKA 6019 Forschungszentrum Karlsruhe
[21] Honda M, Kajita T, Kasahara K, Midorikawa S and Sanuki T 2007 *Phys. Rev. D* **75** 043006
[22] Enberg R, Reno M H and Sarcevic I 2008 *Phys. Rev. D* **78** 043005
[23] Cowan G, Cranmer K, Gross E and Vitells O 2011 *Eur. Phys. J. C* **71** 1554